Carrier-less amplitude and phase modulated visible light communication system based on a constellation-shaping scheme

Zhixin Wang (王智鑫), Mengjie Zhang (张梦洁), Siyuan Chen (陈思源), and Nan Chi (迟 楠)*

State Key Lab of ASIC, Department of Communication Science and Engineering, Fudan University, Shanghai 200433, China

**Corresponding author: nanchi@fudan.edu.cn*

Received July 3, 2016; accepted December 23, 2016; posted online January 22, 2017

In this Letter, we propose a novel constellation-shaping carrier-less amplitude and phase (CAP) modulation scheme to alleviate the systematic nonlinearity in visible light communication (VLC) systems. A simple geometric transformation shaping method is employed to convert the normal square lattice constellation into multiple circular constellations. The feasibility and performance are investigated and experimentally demonstrated by a 1.25 Gb/s CAP-modulated VLC system. The results indicate that the circular constellation has better resistance to systematic nonlinearity compared with a rectangular constellation. The dynamic range of input signal peak-to-peak values promotes 20% at a low bias voltage nonlinear area and 50% at a high bias voltage nonlinear area. To the best of our knowledge, this is the first time constellation-shaping CAP has ever been reported in indoor high data rate VLC systems.

OCIS codes: 060.4080, 060.2605.

doi: 10.3788/COL201715.030602.

Light-emitting diode (LED) -based visible light communication (VLC) systems have been considered as a promising technology for future wireless access due to their unique advantages, such as low cost, low power consumption, lack of license requirement, and high security[1]. A lot of investigations have been carried out for different VLC applications, especially indoor high-speed wireless access[2–7]. To achieve a high data rate and high spectral efficiency (SE), many advanced modulation formats have been demonstrated and utilized in VLC systems, such as carrier-less amplitude and phase (CAP) modulation[5], discrete multi-tone modulation[8], and Nyquist single-carrier modulation[9]. Among them, CAP modulation is considered as a promising technique due to its low complexity and high SE. Recently, an 8 Gb/s VLC system employing high-order CAP modulation has been experimentally demonstrated[10], which is the highest data rate ever achieved in CAP-modulation-based VLC systems. Moreover, post-equalization algorithms, such as cascaded multi-modulus algorithm (CMMA)[11], modified cascaded multi-modulus algorithm (M-CMMA), recursive least square algorithm (RLS), decision directed least mean square algorithm (DD-LMS)[10] have been used to overcome the inter-symbol interference (ISI) for signal recovery in VLC system as well.

It is well known that LEDs have two nonlinear areas at low and high bias voltages. The nonlinearity effect of LEDs will influence the transmission performance[3] and compress the dynamic range of the input signals' peak-to-peak values (Vpp) in the VLC system. Therefore, almost every reported VLC system works in the linear area of an LED. However, the illumination ability is not fully used when the LED works in the low bias voltage linear area. Thus, nonlinearity is considered to be an obstacle to guaranteeing efficient illumination and high-speed communication at the same time. Therefore, it is very necessary to alleviate the impact of nonlinearity and expand the dynamic range to make VLC systems more adaptive to complicated practical user working environments.

In this Letter, to alleviate the systematic nonlinearity, we propose a novel constellation-shaping CAP modulation scheme in an efficient illumination VLC system. A simple geometric transformation shaping method is employed to convert the normal square lattice constellation into multiple circular constellations. The performance of the constellation-shaping scheme has been widely investigated by researchers in areas like wireless communication systems and optical fiber communication[12,13]. However, there are rarely systematic research achievements in VLC systems. To the best of our knowledge, an 8-order quadrature amplitude modulation (8-QAM) constellation shaping techniques have been applied in VLC system shown in Ref. [14]. In Ref. [14], the researchers did a preliminary study on constellation-shaping schemes appropriate for indoor VLC systems with four kinds of 8-QAM specially shaped constellations. A comparison between Ref. [14] and our report is listed in Table 1.

Additionally, the feasibility and performance are experimentally demonstrated by a 1.25 Gb/s CAP-modulated VLC system over 1 m free-space transmission. When considering the 7% forward error correction (FEC) limit of 3.8×10^{-3}, the results indicate that the circular constellation has better resistance to systematic nonlinearity compared with a rectangular constellation, at the cost of about 9.2% extra computational complexity. The dynamic range

Table 1. Differences Between Ref. [14] and Our Report

Items	Ref. [14]	Proposed
QAM order	8-QAM	32-QAM
Modulation formats	Single carrier	CAP
Constellation generation	Regular polygon design	Geometric transformation
Experiment	Yes	Yes
Distance	0.5 m (in door)	1 m (in door)
Comparing group	Four 8-QAM constellations	Two 32-QAM constellations

of the input signal Vpp promotes 20% at the low bias voltage nonlinear area and 50% at the high bias voltage nonlinear area. To the best of our knowledge, this is the first time constellation-shaping CAP has ever been reported in high data rate VLC systems.

In wireless communication systems, constellation shaping is mainly used to reduce the peak ratio and approach the channel capacity limitation[15]. Traditional constellation-shaping technologies divide the constellation points into different sets, and each set corresponds to a sub-constellation. When the transmission probability of low power signals is higher than that of high power signals, the peak ratio of whole signals can be reduced effectively[16].

Different from the traditional shaping method based on collection division, the much simpler geometric transformation shaping method utilizing a series of nonlinear shaping coefficients is employed here[17]. By compressing the high-amplitude constellation point, a normal rectangular constellation will be compressed into multiple circular constellations, thus increasing the average amplitude of all constellation points. Moreover, when the system is amplitude limited, the circular constellation will increase the average output signal power compared with a rectangular constellation under the same signal Vpp.

The formula of forward constellation shaping can be expressed as

$$\begin{cases} x_f = \frac{x_s}{r_s}, y_f = \frac{y_s}{r_s}, r_s = \sqrt{1+\left(\frac{y}{x}\right)^2}; & \text{if } |x_s| \le |y_s| \\ x_f = \frac{x_s}{r_s}, y_f = \frac{y_s}{r_s}, r_s = \sqrt{1+\left(\frac{x}{y}\right)^2}; & \text{if } |x_s| < |x_s| \\ x_f = 0, y_f = 0; & \text{if } x_s \,\&\, y_s = 0 \end{cases}, \quad (1)$$

where x_s, y_s indicate the $X-Y$ axis of the original signal. r_s is the nonlinear shaping coefficient of the transmitter, which is decided by relative relations of x_s, y_s. x_f, y_f indicate the $X-Y$ axis of the shaping signal.

The inverse constellation-shaping formula can be expressed as

$$\begin{cases} x_r = x_n \cdot r_n, y_r = y_n \cdot r_n, r_n = \sqrt{1+\left(\frac{y_n}{x_n}\right)^2}; & \text{if } |x_n| \ge |y_n| \\ x_r = x_n \cdot r_n, y_r = y_n \cdot r_n, r_n = \sqrt{1+\left(\frac{x_n}{y_n}\right)^2}; & \text{if } |x_n| < |y_n| \\ x_r = 0, y_r = 0; & \text{if } x_n \,\&\, y_n = 0 \end{cases}, \quad (2)$$

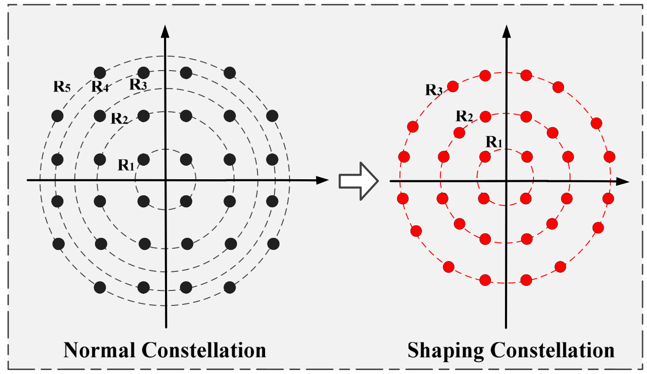

Fig. 1. Constellation of QAM-32 before and after shaping.

where x_n, y_n indicate the $X-Y$ axis of the receiving signal. r_n is the nonlinear inverse shaping coefficient of the receiver, which is decided by relative relations of x_n, y_n. x_r, y_r indicate the $X-Y$ axis of the inverse shaping signal.

Figure 1 shows the constellation of QAM-32 before and after shaping by Eq. (1). It can be found that the high-amplitude constellation point is compressed, and the rectangular constellation is shaped into a circular constellation. Moreover, after shaping, the reference circles are reduced from 5 to 3. The three circles are uniformly distributed, which is the reason for the better resistance to the nonlinearity.

In VLC systems, the systematic nonlinearity mainly is from the amplifier and LEDs, especially the LEDs. Figure 2 shows the *V-I* curve of the red LED used in our experiment. There are two nonlinear areas at low and high voltages, which are about 1.7–2.2 and 3.2–3.8 V. In the nonlinear area, signal distortion by the nonlinearity effect will seriously influence the bit error rate (BER) performance. The high voltage area is our target region for high-speed transmission and efficient illumination of the VLC system in this Letter.

Additionally, the ISI induced by optical multi-path dispersion, the sampling time offset, etc. will seriously degrade the system performance as well. So, a post-equalizer is needed to mitigate the interference and recover the

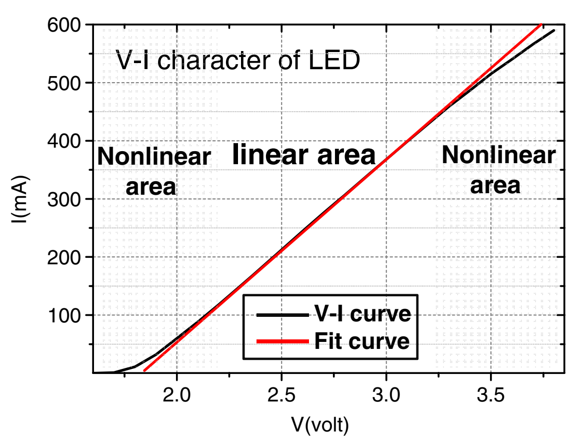

Fig. 2. *V-I* curve of red LED.

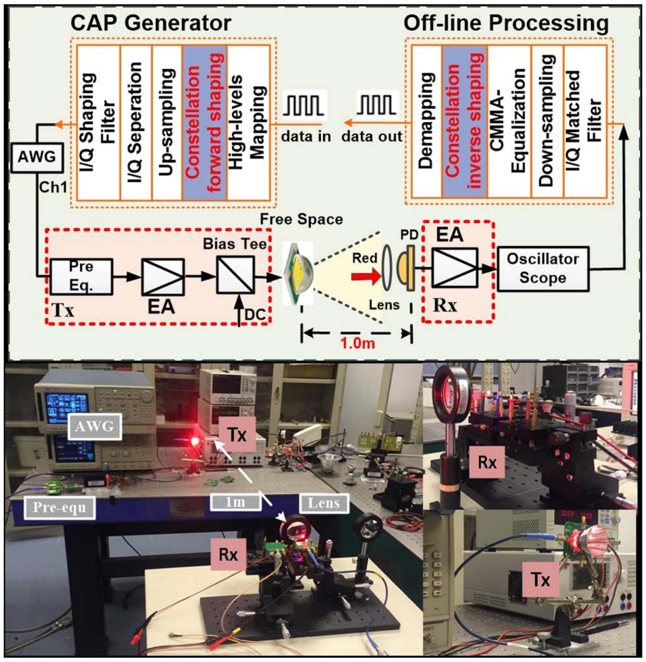

Fig. 3. Experimental setup of the VLC system employing constellation-shaping CAP and CMMA.

signals. A series of post-equalization schemes, such as CMMA[11], M-CMMA, RLS[10], and DD-LMS[11], has been widely investigated and utilized in VLC systems. Among them, the CMMA, as an adaptive equalization algorithm, is especially useful for circular VLC systems due to its quick convergence and modulation transparency. In our experiment, only one CMMA filter is utilize for post-equalization and signal recovery.

Figure 3 shows the experimental setup of the VLC system employing constellation-shaping CAP and CMMA. At the transmitter, the original bit sequence is mapped into 2^N-QAM complex symbols first. The 2^N-QAM signal is sent for constellation shaping. Then, the shaping high-order QAM signal is sent for standard CAP modulation. The details of the CAP modulation and demodulation have been well described in Ref. [18], including the up-sampling, in-phase and quadrature (I/Q) separation, and I/Q shaping filter, which are orthogonal shaping filter pairs. The roll-off coefficient of the square-root raised-cosine function for CAP modulation and demodulation is set at 0.1.

In this experiment, we use a Tektronix AWG 520C to generate the CAP signals. The generated CAP signals are then pre-amplified by a self-designed bridged-T-based pre-equalizer to compensate for the LED frequency attenuation at high frequency components[19,20] so it expands the LED modulation bandwidth. The modulation bandwidth is fixed at 250 MHz. Here, a commercially available RGBY LED (LED Engine, output power: 1 W) is utilized as the transmitter. Through an electrical amplifier (EA, Mini-circuits, 25 dB gain), the electrical signal and DC-bias voltage are combined by a bias tee and used to drive the red-colored chips of the RGBY LED. A reflection

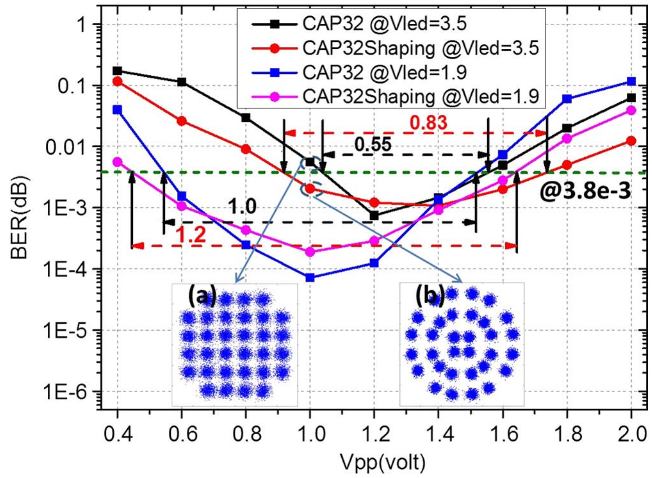

Fig. 4. Measured BER of CAP-32 versus different input signal Vpps at Vleds equal 3.5 and 1.9 V. (a) Constellation of normal QAM-32. (b) Constellation of shaping QAM-32.

cup with a 60° divergence angle is applied to the RGB LED to decrease the beam angle of the LED for longer transmission distances.

After the 1 m free-space transmission, a commercial positive intrinsic-negative (PIN) photodiode (Hamamatsu 10784) is used to detect the optical signals at the receiver. Before the PIN, lenses (50 mm in diameter and with a 50 mm focus length) are used to focus the light. Here, we design a trans-impedance amplifier (TIA) receiving circuit for the PIN, and the outputs of the receiver are amplified by the EAs and then recorded by channel one of a digital storage oscilloscope (Agilent DSO54855A) for further offline demodulation and signal processing.

In offline signal processing, an electrical signal is sent into two digital match filters to separate the in-phase and quadrature components. After down-sampling, the CMMA is used to mitigate the signal ISI. Then inverse constellation shaping and QAM decoder are used to further recover the original bit sequence.

Figure 4 shows the measured BER versus different input signal Vpps when the bias voltages (Vled) equal 3.5 and 1.9 V. Figures 4(a) and 4(b) show the constellation of the normal QAM-32 and the shaping QAM-32, respectively. We know from Fig. 2 that Vleds equal to 3.5 and 1.9 V are the nonlinear areas of the used LED. It can be found from Fig. 4 that when the Vled is fixed at 1.9 V, the dynamic ranges of the normal CAP-32 and the shaping CAP-32 are 1.0 and 1.2 V, respectively, which indicate a 20% improvement. When the Vled is fixed at 3.5 V, the dynamic ranges of the normal CAP-32 and the shaping CAP-32 are 0.55 and 0.83 V, respectively, which indicate a 50% improvement.

It should be noted that the best BER performance of the normal CAP-32 is better than that of the shaping CAP-32 at Vleds equal to 3.5 or 1.9 V. This can be explained by Fig. 1: the Euclidean distance of the shaping constellation is reduced, which will surely degrade the system performance. Therefore, it is worth noting that alleviation of

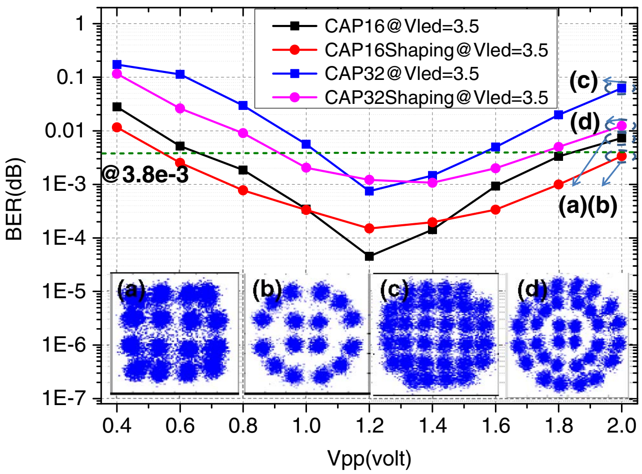

Fig. 5. Measured BER of CAP-32 and CAP-16 versus different input signal Vpps at a Vled equal 3.5 V. (a) CAP-16, (b) shaping CAP-16, (c) CAP-32, and (d) shaping CAP-32.

the nonlinear effect is at the cost of a reduced Euclidean distance. So, the shaping CAP is more suitable for high-efficient illumination scenarios where the dynamic range is more important. Besides, the modulation bandwidth is fixed at 250 MHz; therefore, the transmission data rate of $250 \times 5 = 1.25$ Gb/s is successfully achieved at a distance of 1 m.

Figure 5 shows the measured BERs of CAP-32 and CAP-16 versus different input signal Vpps while the Vled is fixed at 3.5 V. It can be seen that CAP-16 and CAP-32 have the same result of a wider dynamic range after shaping. Moreover, Figs. 5(a)–5(d) show the constellation of CAP-16 and CAP-32 influenced by the nonlinear effect when the Vpp equals 2.0 V. As shown in Figs. 5(a) and 5(b), it is clear that the constellation of the normal CAP-16 is seriously distorted, while the shaping CAP-16 keeps a stable circular structure. The same result can be found by comparing Figs. 5(c) and 5(d) as well.

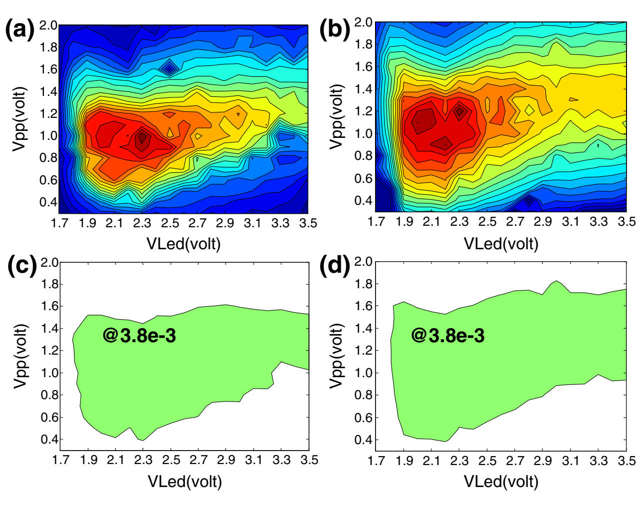

Fig. 6. Measured BER performance and working range of CAP-32 versus different Vleds and Vpps (a,c) without constellation shaping, and (b,d) with constellation shaping.

Figures 6(a) and 6(b) show the measured BER performance versus the different Vled and Vpp of the normal CAP-32 and shaping CAP-32, respectively. Figures 6(c) and 6(d) shows the working range versus the Vled and Vpp in terms of a 7% FEC limit of 3.8×10^{-3}. It can be found from Figs. 6(a) and 6(b) that the optimal working point of the shaping CAP-32 is slightly higher than that of the normal CAP-32. Moreover, by comparing Figs. 6(c) and 6(d), it is obvious that the shaping CAP-32 has a wider working range over the whole Vled and Vpp scope. With the bias voltage increasing, the dynamic range of the shaping CAP-32 decreases slowly and the Vpp shifts upward in order to maintain modulation depth. In a word, shaping CAP can support a wider working range, especially under high voltage. This means the shaping CAP will be more stable in the scenarios of high-speed and high-efficiency illuminated VLC communications system.

In conclusion, we propose and experimentally demonstrate the performance of a novel constellation-shaping CAP modulation scheme in a VLC system in this Letter. The feasibility is experimentally demonstrated by a 1.25 Gb/s CAP-based VLC system. The results indicate that the proposed constellation-shaping scheme can alleviate the systematic nonlinearity compared with a normal constellation. Additionally, the dynamic range of the input signal Vpp is promoted 20% at the low bias voltage nonlinear area and 50% at the high bias voltage nonlinear area. To the best of our knowledge, this is the first time constellation-shaping CAP has ever been reported in VLC systems, and the results prove its potential in future high-speed efficient illumination VLC systems.

References

1. D. O'Brien, H. L. Minh, L. Zeng, G. Faulkner, K. Lee, D. Jung, Y. Oh, and E. T. Won, Proc. SPIE **7091**, 709106 (2008).
2. R. Li, Y. Wang, C. Tang, Y. Wang, H. Shang, and N. Chi, Chin. Opt. Lett. **11**, 080605 (2013).
3. K. Ying, Z. Yu, R. J. Baxley, H. Qian, G.-K. Chang, and G. T. Zhou, IEEE Wireless Commun. **22**, 36 (2015).
4. Y. Wu, A. Yang, L. Feng, and Y. Sun, Chin. Opt. Lett. **11**, 030601 (2013).
5. Y. Wang, X. Huang, L. Tao, J. Shi, and N. Chi, Opt. Express **23**, 13626 (2015).
6. J. Luo, Y. Tang, H. Jia, Q. Zhu, and W. Xue, Chin. Opt. Lett. **14**, 120604 (2016).
7. H. Li, Y. Zhang, X. Chen, C. Wu, J. Guo, Z. Gao, and H. Chen, Chin. Opt. Lett. **13**, 080605 (2015).
8. J. Sung, C. Chow, and C. Yeh, Opt. Express **22**, 7538 (2014).
9. Y. Wang, X. Huang, J. Zhang, Y. Wang, and N. Chi, Opt. Express **22**, 15328 (2014).
10. Y. Wang, L. Tao, X. Huang, J. Shi, and N. Chi, IEEE Photon. J. **7**, 1 (2015).
11. L. Tao, Y. Ji, J. Liu, A. P. T. Lau, N. Chi, and C. Lu, IEEE Network **27**, 6 (2013).
12. C. Thomas, M. Weidner, and S. Durrani, IEEE Trans. Commun. **22**, 168 (1974).

13. M. Nölle, F. Frey, R. Elschner, C. Schmidt-Langhorst, A. Napoli, and C. Schubert, in *Optical Fiber Communication Conference* (Optical Society of America, 2014), paper W3B-2
14. J. Zhao, C. Qin, M. Zhang, and N. Chi, Photon. Res. **4**, 249 (2016).
15. H. Kwok and D. Jones, in *Proceedings of IEEE International Symposium on Information Theory* (IEEE, 2000).
16. S. A. Tretter, *Constellation Shaping, Nonlinear Precoding, and Trellis Coding for Voiceband Telephone Channel Modems: With Emphasis on ITU-T Recommendation* (2012), Vol. **34**.
17. M. Yankov, S. Forchhammer, K. J. Larsen, and L. P. Christensen, in *IEEE International Conference on Communications (ICC)* (IEEE, 2014), p. 2112.
18. L. Tao, Y. Wang, Y. Gao, A. P. T. Lau, N. Chi, and C. Lu, Opt. Express **21**, 6459 (2013).
19. X. Huang, S. Chen, Z. Wang, J. Shi, Y. Wang, J. Xiao, and N. Chi, IEEE Photon. J. **7**, 1 (2015).
20. X. Huang, S. Chen, Z. Wang, Y. Wang, and N. Chi, Chin. Opt. Lett. **13**, 100602 (2015).